

# CHEMISTRY

---

## AN ASIAN JOURNAL

www.chemasianj.org

### Accepted Article

**Title:** Coordination Chemistry of Bis-Cyclic Alkyl(Amino) Carbene (cAAC)-Supported Di-Phosphorus (P<sub>2</sub>): An Efficient Route to Elusive Di-Phosphorus-Monoxide(P<sub>2</sub>O)-Gold Complex

**Authors:** Maria Francis, Ekta Nag, and Sudipta Roy

This manuscript has been accepted after peer review and appears as an Accepted Article online prior to editing, proofing, and formal publication of the final Version of Record (VoR). The VoR will be published online in Early View as soon as possible and may be different to this Accepted Article as a result of editing. Readers should obtain the VoR from the journal website shown below when it is published to ensure accuracy of information. The authors are responsible for the content of this Accepted Article.

**To be cited as:** *Chem. Asian J.* **2023**, e202300882

**Link to VoR:** <https://doi.org/10.1002/asia.202300882>

A Journal of



---

WILEY-VCH

# Coordination Chemistry of Bis-Cyclic Alkyl(Amino) Carbene (cAAC)-Supported Di-Phosphorus (P<sub>2</sub>): An Efficient Route to Donor Base-Stabilized Elusive Di-Phosphorus-Monoxide(P<sub>2</sub>O)-Gold Complex

Maria Francis,<sup>[a]</sup> Ekta Nag,<sup>[a]</sup> and Sudipta Roy\*<sup>[a]</sup>

[a] M. Francis, E. Nag, Dr. S. Roy  
Department of Chemistry, Indian Institute of Science Education and Research (IISER) Tirupati,  
Tirupati 517507, India  
E-mail: [roy.sudipta@iisertirupati.ac.in](mailto:roy.sudipta@iisertirupati.ac.in)  
Homepage: <https://sudiptagroup.com/>

Supporting information for this article is given via a link at the end of the document.

**Abstract:** The stability and reactivity studies of heavier di-atomic group-15 congeners of alkynes, e.g., the di-phosphorus (P≡P) compounds have been the topic of huge interest because of their contrasting transient properties and lower stability compared to those of the stable molecular di-nitrogen (N≡N). Herein, we depict the reactivity studies of the bis-cAAC-stabilized di-phosphorus (P<sub>2</sub>) having an inversely polarized phosphalkene nature featuring the C=P double bonds with Au(I)Cl. Both the mono-, and the di-aurated phosphalkenes with the formulae [(Me<sub>2</sub>-cAAC=P)<sub>2</sub>(AuCl)] (**2**), and [(Me<sub>2</sub>-cAAC=P)<sub>2</sub>(AuCl)<sub>2</sub>] (**3**), respectively have been isolated in the solid state. Moreover, for the first time, we have been able to isolate the cAAC-stabilized tetra-aurated elusive di-phosphorus-monoxide (P<sub>2</sub>O) in the solid state with the formula [(Cy-cAAC=P)-O-(P=cAAC-Cy)(AuCl)<sub>4</sub>] (**5**) in presence of oxygen. Complexes **2-3**, **5** have been structurally characterized by single crystal X-ray diffraction, and further studied by NMR spectroscopy. Our findings reveal significant elongation of the C<sub>cAAC</sub>-P bonds in complexes **2-3**, **5**, and the presence of aurophilic interaction in **5**. Quantum chemical calculations, including density functional theory (DFT), and energy decomposition analysis coupled with natural orbitals for chemical valence (EDA-NOCV) have been performed to study the electron densities distribution and nature of bonding in **2-3**, **5**.

## Introduction

The neutral monomeric di-phosphorus with a classical P≡P triple bond is a highly reactive species compared to its lighter congener, the molecular di-nitrogen N<sub>2</sub>, which is only observed either in the gas phase at an elevated temperature or by the matrix isolation method.<sup>[1]</sup> The attempts to stabilize, and isolate P<sub>2</sub> in the solid state by using Lewis bases, e.g., the carbenes (N-heterocyclic carbenes (NHCs), cyclic alkyl(amino) carbenes (cAAC)) led to the reduction of the overall bond order due to charge transfer to the π\* orbitals of the electrophilic P<sub>2</sub> moiety.<sup>[2]</sup> On the other hand, P<sub>2</sub> on its own behaves as a Lewis base under the coordination sphere of transition metals because of the presence of the lone pair of electrons and thereby retains the multiple bonds between the two P atoms.<sup>[3]</sup> In 2008, Robinson and co-workers first reported the N-heterocyclic carbene (NHC, L<sub>2</sub>)-stabilized P<sub>2</sub> molecules L:P=P:L, **A** (L: = :C{N(2,6-*i*-Pr<sub>2</sub>C<sub>6</sub>H<sub>3</sub>)CH<sub>2</sub>)}<sub>2</sub>) and :C{N(2,4,6-Me<sub>3</sub>C<sub>6</sub>H<sub>2</sub>-CH<sub>2</sub>)}<sub>2</sub> in 21%-56% of yields exhibiting the unique bis-phosphinidene structure containing two singly bonded P atoms, each with two lone pairs of electrons, and the dative C:→P bonds.<sup>[2a]</sup> **A** was synthesized

by the reduction of the adduct NHC:PCl<sub>3</sub> using KC<sub>8</sub> as the reducing agent (Figure 1). In 2009, Bertrand and co-workers isolated the cyclic alkyl(amino) carbene (cAAC)-stabilized 2,3-diphosphabutadiene **B**, an inversely polarized phosphalkene<sup>[4]</sup> shown in Figure 1 having the formal P=C double bonds in only 12% yield by treating cAAC with white phosphorus (P<sub>4</sub>).<sup>[2b]</sup> Later on, Driess and co-workers reported on the synthesis of an NHC-stabilized bis-phosphinidene **C** via the reduction of a bis-phosphine precursor in a comparatively higher yield (60%, Figure 1).<sup>[2c]</sup> Moreover, they successfully utilized **C** as a chelating ligand for the first time in order to stabilize various mono- and multi-metallic systems exploiting the available lone pairs on the P atoms. In 2020, the same group reported the stabilization of P<sub>2</sub> (**D**) by utilizing the strongly chelating σ-donor bis-silylene (NHSi) ligand (Figure 1).<sup>[2d]</sup>

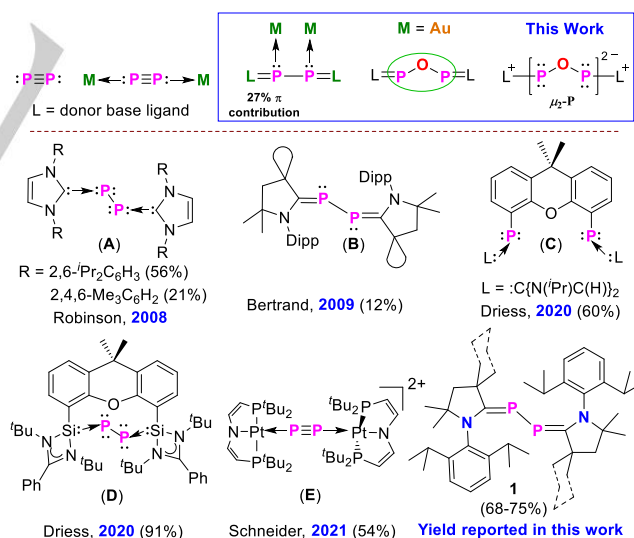


**Figure 1.** Top: Different bonding modes of P<sub>2</sub>. Bottom: Previously reported bis-phosphorus (P<sub>2</sub>) compounds (**A-E**). The % yields are mentioned in parenthesis.

Based on the availability of the lone pairs of electrons on P atoms, the donor base-stabilized P<sub>2</sub> molecules can behave as potential four-, six-, or eight-electron donor ligands, coordinating to various transition metals.<sup>[5]</sup> Cummins and co-workers reported the thermal extrusion of P<sub>2</sub> from the niobium diphosphaazide complexes,<sup>[6]</sup> and the Pt(0) complex (C<sub>2</sub>H<sub>4</sub>)Pt(PPh<sub>3</sub>)<sub>2</sub>, which further coordinated to the electronically unsaturated W(CO)<sub>5</sub> to form the corresponding complexes.<sup>[7]</sup> So far, the coordination

chemistry of the bis-NHC-stabilized di-phosphorus (**A**) having phosphinidene character have been explored to some extent by treating it with Lewis acidic species, e.g.,  $\text{BH}_2^+$  (**F**),  $\text{H}^+$  (Figure 2).<sup>[8]</sup> On the other hand, the reduction of **A** resulted in the formation of the lithiated NHC-phosphinidene adduct  $\text{L:P-H}$  (**J**,  $\text{L} = \text{:C}(\text{N}(2,6\text{-iPr}_2\text{C}_6\text{H}_3)_2\text{CHCl})(\text{THF})_3$ ) (Figure 2).<sup>[9]</sup> In 2010, Bertrand's group isolated the  $\text{P}_2$  radical cation **I**, and the corresponding di-cation exploiting the electron-rich  $\text{P}_2$  fragments in species **A** and **B** considering their corresponding phosphinidene forms, which can easily undergo oxidation (Figure 2).<sup>[2b]</sup> In 2013, Robinson's group also isolated the carbene-stabilized di-phosphorus tetroxide  $\text{O}_2\text{P-PO}_2$  (**G**), a formal oxidized form of  $\text{P}_2$  (Figure 2).<sup>[10]</sup> In contrast with nitrogen, which readily forms a series of stable, isolable oxides, e.g.,  $\text{NO}$ ,  $\text{NO}_2$ ,  $\text{N}_2\text{O}_x$  ( $x = 1, 3, 4, 5$ ),<sup>[11]</sup> the corresponding phosphorus analogs, i.e.,  $\text{PO}$ ,  $\text{PO}_2$ ,  $\text{P}_2\text{O}_x$  ( $x = 1, 3, 4, 5$ ) are highly reactive, and so far, studied only in the gas phase or by low-temperature matrix isolation methods.<sup>[12]</sup> As a result, the synthetic routes for these reactive phosphorus oxides are scarce in the literature. The phosphorus monoxide ( $\text{PO}$ ), and di-phosphorus monoxide ( $\text{P}_2\text{O}$ ) were first stabilized in the form of their transition metal complexes.<sup>[13-14]</sup> However, alternative synthetic strategies employing main group elements are yet to be explored.

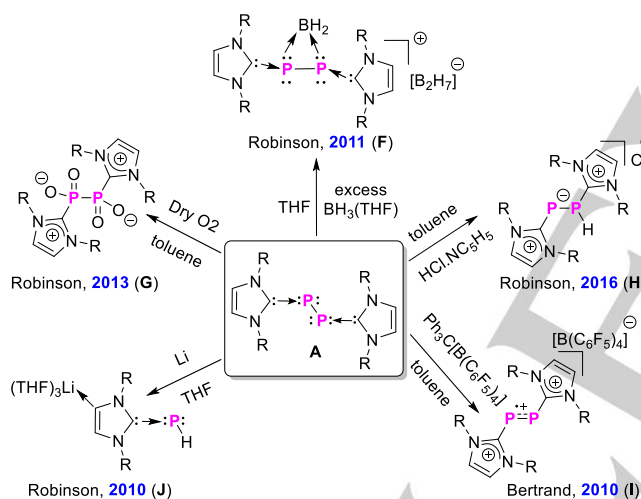


**Figure 2.** Reactivity studies of bis-NHC-stabilized di-phosphorus ( $\text{P}_2$ ) compound (**A**).

Although, there have been various reports on the reactivity of bis-NHC-stabilized  $\text{P}_2$ , the same for the analogous cAAC-stabilized  $\text{P}_2$  (**1**) is extremely rare so far, presumably due to the comparatively lower yield obtained by the reported synthetic route.<sup>[2b]</sup>

Herein, we report on a new straight-forward synthetic route for the bis-cAAC-stabilized di-phosphorus ( $\text{cAAC=P}_2$ ) (**1**)<sup>[2b]</sup> with an improved yield by the deductive de-halogenation of a concentrated solution of the chloro-phosphinidenes  $\text{cAAC=P-Cl}$ <sup>[15]</sup> using K metal under ambient reaction conditions. Further, we studied the coordination behavior of **1** with  $\text{AuCl}$  under Ar atmosphere, and in the presence of aerial oxygen to isolate the mono- and di-aurated di-phosphorus complexes  $[(\text{Me}_2\text{-cAAC=P})_2(\text{AuCl})]$  (**2**),  $[(\text{Me}_2\text{-cAAC=P})_2(\text{AuCl})_2]$  (**3**), and the tetra-aurated complex of the first carbene-stabilized di-phosphorus

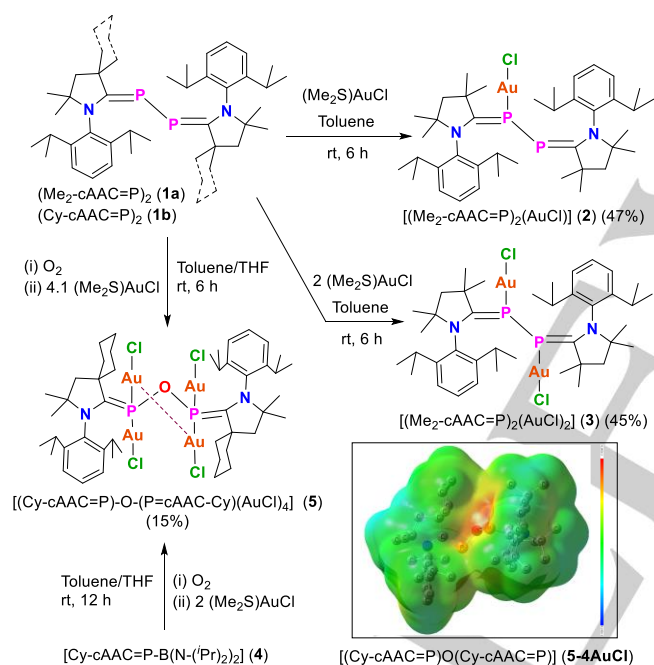
monoxide  $[(\text{Cy-cAAC=P})\text{-O-(P=cAAC-Cy)(AuCl)}_4]$  (**5**), respectively in moderate to good yields.

## Results and Discussion

Previously, we have reported that the chloro-phosphinidene  $\text{cAAC=P-Cl}$ <sup>[15]</sup> can be quantitatively converted to the corresponding K-phosphinidenide,  $\text{cAAC=P-K}$  by reductive dehalogenation of the former in the presence of two equiv of K-metal under ambient temperature.<sup>[16]</sup>  $\text{cAAC=P-K}$  can be inherently utilized as the source of the mono-anionic phosphorus ligand,  $\text{cAAC=P}^-$ ,<sup>[17-18]</sup> which can bridge between two or three metal centres; where cAAC acts as the electron reservoir. In this study, we show that  $\text{cAAC=P-Cl}$  can also be efficiently utilized as the precursor for the synthesis of cAAC-stabilized di-phosphorus ( $\text{cAAC=P}_2$ ) (**1**) by tuning the concentration of the reaction mixture. A 1:1 molar mixture of  $\text{cAAC=P-Cl}$  and K metal was stirred in THF (concentrated reaction solution) at room temperature (rt) for 6-12 h until the color of the reaction solution turned golden yellow to greenish-yellow. Afterward, the reaction mixture was filtered to remove KCl, and the filtrate was concentrated to dryness under reduced pressure. The resulting greenish-yellow solid was extracted in *n*-hexane, and the concentrated solution was stored in a refrigerator at 0 °C for 7-8 days to obtain long yellow rods of **1a** ( $(\text{Me}_2\text{-cAAC=P})_2$ , 68%), and **1b** ( $(\text{Cy-cAAC=P})_2$ , 75%), which were characterized by NMR spectroscopy (see SI).<sup>[2b,17]</sup> Based on the quantum chemical calculations we have previously shown that in the presence of K metal,  $\text{cAAC=P-Cl}$  undergoes reductive dehalogenation resulting in the formation of the high energy intermediate  $\text{cAAC=P}^\cdot$  radical (-37.0 kcal/mol), which can go into two competing pathways: the first one is the highly probable dimerization to produce  $(\text{cAAC=P})_2$  (-30.3 kcal/mol), and the other one is the second electron transfer from K (-45.5 kcal/mol) to produce the corresponding phosphinidenide ( $\text{cAAC=P-K}$ ).<sup>[16]</sup>

As a part of our continuous research efforts,<sup>[20]</sup> we next aimed to study the reactivity of  $(\text{cAAC=P})_2$ , **1** (**1a** =  $\text{Me}_2\text{-cAAC}$ ; **1b** =  $\text{Cy-cAAC}$ ) with  $(\text{Me}_2\text{S})\text{AuCl}$  to probe the availability of the coordinating lone pairs of electrons on the P atoms in **1**. The reaction of a 1:1 molar ratio of **1a** and  $(\text{Me}_2\text{S})\text{AuCl}$  in toluene at rt for 6 h resulted in a clear orange solution, which was further stirred for 12 h in the absence of light. The reaction solution was then concentrated under reduced pressure, and the orange sticky solid obtained was extracted in anhydrous DCM. The orange blocks of the mono-aurated phosphalkene  $[(\text{Me}_2\text{-cAAC=P})_2(\text{AuCl})]$  (**2**), suitable for X-ray single-crystal diffraction were obtained from the concentrated DCM solution stored at a -32 °C freezer after 4-5 days in 47% yield (Scheme 1). Similarly, when the phosphalkene **1** was treated with  $(\text{Me}_2\text{S})\text{AuCl}$  in a 1:2 molar ratio, the corresponding di-aurated phosphalkene  $[(\text{Me}_2\text{-cAAC=P})_2(\text{AuCl})_2]$  (**3**) was obtained in 45% yield as golden yellow blocks, suitable for X-ray single-crystal diffraction after 3-5 days from a concentrated DCM solution stored at -32 °C in a freezer (Scheme 1). The  $^{31}\text{P}$  NMR spectroscopic analyses of the crude reaction mixtures for both 1:1 and 1:2 (compound **1a**: $(\text{Me}_2\text{S})\text{AuCl}$ ) reactions showed the formation of only complexes **2**, and **3**, respectively along with the presence of **1a**

even after 12 h of reaction time. A prolonged reaction time could not improve the yields of **2/3**. Moreover, the formation of a mixture of complexes (**2**, and **3**) or any other products were not observed. On the other hand, when one equiv of the previously reported boryl-phosphaalkene [Cy-cAAC=P-B(N-(*i*-Pr)<sub>2</sub>)<sub>2</sub>] (**4**)<sup>[17]</sup> was treated with two equiv of (Me<sub>2</sub>S)AuCl in toluene at rt for 12 h, a brownish-orange precipitate was obtained. The reaction mixture was then filtered, and the brownish-orange precipitate obtained was washed with *n*-hexane and dissolved in THF to obtain a golden-yellow solution. The solution was concentrated, exposed to air for a few seconds, and then stored at -32 °C in a freezer. The golden yellow blocks of the complex [(Cy-cAAC=P)-O-(P=cAAC-Cy)(AuCl)<sub>4</sub>] (**5**), suitable for X-ray single-crystal diffraction were obtained in 15% yield after 7-10 days (Scheme 1). A similar product (**5**) was also obtained when the bis-cAAC-supported phosphalkene **1b** was treated with (Me<sub>2</sub>S)AuCl in 1:4 molar ratio in toluene for 12 h at rt in the presence of molecular oxygen, which was confirmed by the <sup>31</sup>P NMR spectrum. However, several attempts to produce single crystals of complex **5** from this reaction mixture were not fruitful.



**Scheme 1.** Syntheses of complexes [(Me<sub>2</sub>-cAAC=P)<sub>2</sub>(AuCl)] (**2**), [(Me<sub>2</sub>-cAAC=P)<sub>2</sub>(AuCl)<sub>2</sub>] (**3**), and [(Cy-cAAC=P)-O-(P=cAAC-Cy)(AuCl)<sub>4</sub>] (**5**). Inset: MEP plot (computed at iso-density surface value of 0.0004 a.u.) of [(Cy-cAAC=P)-O-(P=cAAC-Cy)(AuCl)<sub>4</sub>]-4AuCl (**5-4AuCl**).

The orange to golden yellow crystalline solids of complexes **2-3**, **5** were found to be stable for more than six months under argon atmosphere at rt. The powder of **2**, and **3** melted at 194-196 °C, and 170-172 °C, respectively under an inert atmosphere. The single crystals of **2** were soluble in polar organic solvents, e.g., THF and DCM, but not in non-polar solvents, such as toluene and *n*-hexane. The DCM solution of **2** was found to be stable for months at rt under an argon atmosphere. Complexes **2-3**, and **5** were characterized by NMR spectroscopy. The <sup>31</sup>P NMR spectra of the DCM-*d*<sub>2</sub> solutions of complexes **2**, and **3** exhibited two doublets at 36.2 (*J*<sub>P-H</sub> = 294.8 Hz), -4.1 (*J*<sub>P-H</sub> = 312.1 Hz) ppm,

and a singlet at 14.8 ppm, respectively, which are upfield shifted when compared to the singlets obtained for the bis-phosphaalkene **1a** (55.6 ppm), Me<sub>2</sub>-cAAC=PCl (161.9 ppm), and the corresponding phosphinidene Me<sub>2</sub>-cAAC=P-K (207.3 ppm). On the other hand, the <sup>31</sup>P NMR spectrum of complex **5** exhibited a singlet at -80.9 ppm, which is upfield shifted when compared to those of complex **2**, bis-phosphaalkene **1b** (58.6 ppm), Cy-cAAC=PCl (163.3 ppm), and the corresponding phosphinidene Cy-cAAC=P-K (206.9 ppm), and the bis-carbene-stabilized di-phosphorus-tetraoxide (**G**, 5.8 ppm).

The UV-Vis absorption spectra of complexes **2**, and **3** in DCM exhibited the absorption maxima (λ<sub>max</sub>) at 432, and 425, respectively, which are in good agreement with the computed values (425 nm for **2**, 422 nm for **3**) obtained by the TD-DFT calculations performed on complexes **2**, **3** at BP86/def2-TZVPP level of theory.

The molecular structures of **2-3** have been confirmed by the single-crystal X-ray diffraction (Figures 3-4). **2** crystallizes in the triclinic crystal system with *P*-1 space group. The asymmetric unit of **2** further consists of one lattice DCM molecule. The molecular structure of **2** reveals that the central P(AuCl)P unit is bonded to one Me<sub>2</sub>-cAAC at each of the P atoms confirming the formation of the 1:1 AuCl-adduct with **1**. Both the cAAC ligands are arranged in *trans*-fashion compared to the central P-P bond with the torsion angle of 143.6(1)° (C12-P2-P1-C20). The P-P bond in **2** is found to be 2.181(1) Å, which is very similar to the bis-phosphaalkene **1** ((cAAC)<sub>2</sub>P<sub>2</sub>) (2.184(3) Å),<sup>[2b]</sup> but slightly longer than that of the reported mono-aurated diphosphene (Mes\*{AuCl}P=PMe\*) (Mes = 2,4,6-trimethylphenyl) (1.975(5) Å).<sup>[19]</sup> The C12-P2 and C20-P1 bond lengths are 1.743(2), and 1.757(3) Å, respectively. This is significantly shorter than the bis-phosphaalkene **1** (1.719(7) Å),<sup>[2b]</sup> but strongly in agreement with the chloro-phosphinidene (cAAC)PCl (1.7513(15) Å)<sup>[15]</sup> referring to a donor-acceptor type bond. The bond lengths between the Au and P atoms, and Au and Cl atoms are comparable to those of the previously isolated gold-phosphine complexes.<sup>[21-24]</sup> The sum of the bond angles around the aurated P1 centre is 333.38°. The P1-Au1-Cl1 bond angle in **2** (176.17(3)°) is found to be similar to those of the regular terminal binding of AuCl molecule.

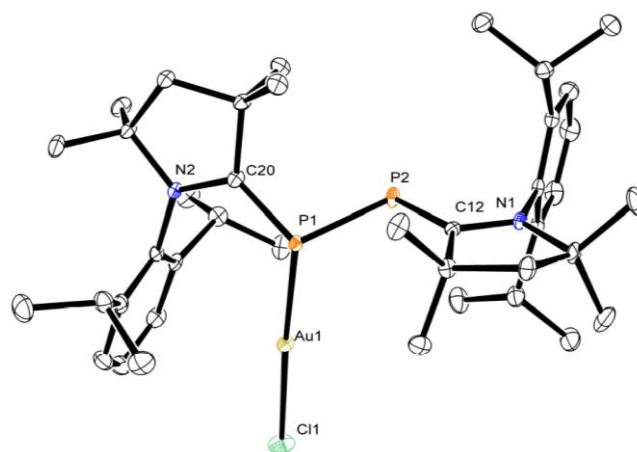


**Figure 3.** Molecular structure of complex [(Me<sub>2</sub>-cAAC=P)<sub>2</sub>(AuCl)] **2**. The anisotropic displacement parameters are depicted at the 50% probability level. Hydrogen atoms and DCM (solvent) are omitted for clarity. Selected experimental [calculated at BP86/def2-TZVPP] bond lengths [Å] and bond

angles [°]: N2–C20 1.337(3) [1.350], P1–C20 1.758(2) [1.751], P1–P2 2.1807(8) [2.184], P2–C12 1.743(2) [1.750], Au1–Cl1 2.3024(6) [2.321], Au1–P1 2.2552(6) [2.262], N1–C12 1.348(3) [1.361]; C20–P1–Au1 118.58(8) [105.89], C12–P2–P1 104.71(8) [102.47], P1–Au1–Cl1 176.17(3) [175.27].

Complex **3** crystallizes in *P*-1 space group. The molecular structure of **3** consists of a central (PAuCl)<sub>2</sub> unit supported by the Me<sub>2</sub>-cAAC ligands, which are arranged in *cis* fashion with respect to the central (PAuCl)<sub>2</sub> unit. The C<sub>cAAC</sub>–P bond lengths are found to be 1.767(5), and 1.760(5) Å, which are slightly longer than the mono-aurated complex **2** (1.743(2), and 1.757(3) Å), and longer than those of the bis-phosphaalkene **1** ((cAAC)<sub>2</sub>P<sub>2</sub>) (1.719(7) Å).<sup>[2b]</sup> The P–P bond distance of **3** (2.163(1) Å) is very close to those of **2** (2.181(1) Å), and **1** (2.184(3) Å).<sup>[2b]</sup> The P3–Au2 (2.250(1) Å), and P2–Au1 (2.240(1) Å) bond lengths are found to be comparable to those of complex **2**, and the previously reported gold-phosphine complexes.<sup>[21–24]</sup> The distance between two Au-centres [Au1⋯Au3] in **3** is 4.017(9) Å, which is too long to be considered an auriphilic interaction [2.50–3.50 Å].<sup>[25]</sup>

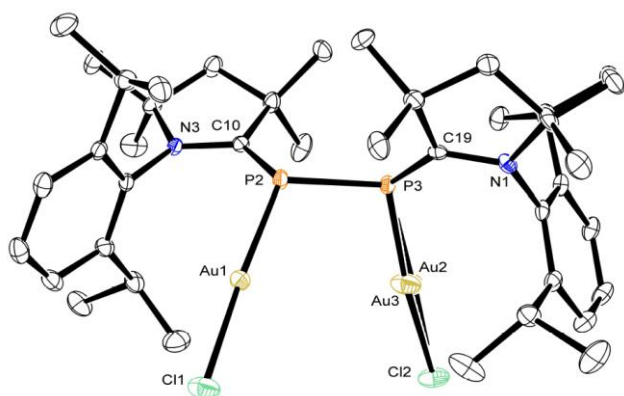


**Figure 4.** Molecular structure of complex [(Me<sub>2</sub>-cAAC=P)<sub>2</sub>(AuCl)<sub>2</sub>] **3**. The anisotropic displacement parameters are depicted at the 50% probability level. Hydrogen atoms are omitted for clarity. Occupancies on Au2 and Au3 are 92% and 8% respectively. Selected experimental [calculated at BP86/def2-TZVPP] bond lengths [Å] and bond angles [°]: N3–C10 1.338(5) [1.340], P2–C10 1.760(4) [1.764], Au1–P2 2.2397(11) [2.254], P3–C19 1.768(4) [1.764], N1–C19 1.331(6) [1.340], Au1–Cl1 2.2924(12) [2.317], Au2–Cl2 2.2999(13) [2.317], Au2–P3 2.2498(13) [2.254], C10–P2–P3 105.39(15) [103.04], and C19–P3–P2 105.73(15) [103.04].

Complex **5** crystallizes in the orthorhombic crystal system with *Pbcn* space group (Figure 5). The molecular structure of **5** is composed of two Cy-cAAC ligands connected by the bis-oxophosphinidene bridge, POP with two AuCl moieties coordinated to each phosphorus atom. Notably, the proximity of Au2 and Au4 atoms results in a semi-supported auriphilic interaction,<sup>[25]</sup> with a close contact distance of 3.1967(6) Å. In the crystal structure of **5**, the P–O bond lengths are determined to be 1.663(7) and 1.656(7) Å, while the P–O–P bond angle measures 116.3(4)°. The P atoms exhibit tetrahedral coordination geometry with four coordinated ligands. The Au–P bond lengths are slightly longer when the Au atoms are involved in the auriphilic interaction (Au4–P2: 2.245(2), Au2–P1: 2.249(2) Å). Importantly, all the observed Au–P bond distances fall within the range of the previously reported gold-phosphorus complexes featuring the POP bridge.<sup>[26]</sup> In comparison with **1** ((cAAC)<sub>2</sub>P<sub>2</sub>),<sup>[2b]</sup> a notable

elongation of the C–P bond lengths (1.850(10) and 1.843(9) Å) is observed in complex **5**.

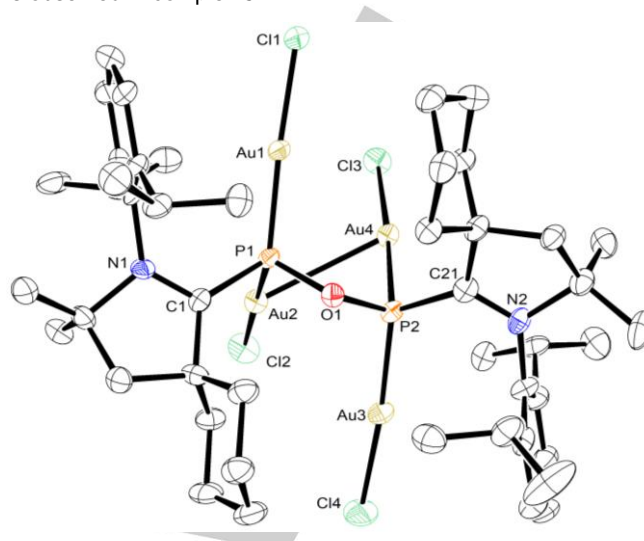


**Figure 5.** Molecular structure of complex **5** [(Cy-cAAC=P)–O–(P=cAAC-Cy)(AuCl)<sub>4</sub>]. The anisotropic displacement parameters are depicted at the 50% probability level. Hydrogen atoms and THF molecule (solvent) are omitted for clarity. Selected experimental [calculated at BP86/def2-TZVPP] bond lengths [Å] and bond angles [°]: Au4–Au2 3.1967(6) [3.092], Au4–P2 2.245(2) [2.259], Au1–P1 2.219(2) [2.231], Au2–P1 2.249(2) [2.259], Au3–P2 2.219(3) [2.231], P2–O1 1.663(7) [1.674], P2–C21 1.850(10) [1.819], P1–O1 1.656(7) [1.674], P1–C1 1.843(9) [1.819], O1–P2–C21 100.6(4) [100.9], P1–O1–P2 116.3(4) [115.0], O1–P1–C1 100.8(4) [100.9].

These values are consistent with the C–P single bond lengths observed in NHC–P(O)<sub>2</sub>–P(O)<sub>2</sub>–NHC (1.895(3) Å)<sup>[27]</sup> and the NHC adduct of PCl<sub>3</sub> (1.871(11) Å).<sup>[8]</sup> The structure of the complex [(Cy-cAAC=P)–O–(P=cAAC-Cy)(AuCl)<sub>4</sub>] **5** can finally be considered as the bis-cAAC stabilized tetra-AuCl adduct of diphosphorus monoxide (P<sub>2</sub>O).

## Computational Studies

We have performed density functional theory (DFT) calculations, and Energy decomposition analysis coupled with natural orbital for chemical valence (EDA-NOCV) to have a deeper understanding of the nature of participating orbitals of the bis-cAAC-stabilized P<sub>2</sub> (**1**) in complex formation, along with the electron densities distribution and bonding analyses of the isolated complexes **2–3**, **5**. Geometry optimization of the complexes **2–3**, **5** was carried out at the BP86-D3(BJ)/def2-TZVPP<sup>[28]</sup> level of theory, and the theoretical bond parameters obtained were found to be in good agreement with the experimental values (see SI). The optimized structures of complexes **2–3** revealed that there was no significant change in the P–P bond lengths after the mono- and di-auration of the cAAC-stabilized bis-phosphaalkene **1** (2.184(3) Å).<sup>[2b]</sup> The natural bond orbital (NBO) analysis<sup>[29]</sup> was conducted on the optimized coordinates of compound **1**, and complexes **2–3**, **5**, employing the BP86-D3(BJ)/def2-TZVPP level of theory. The NBO analysis of compound **1** indicated the presence of a lone pair on each of the P atoms, facilitating the coordination to AuCl moiety. The HOMO-LUMO gaps of **2–3**, and **5** were determined

to be 2.06, 2.21, and 1.71 eV, respectively. For complex **2**, two distinct bonding occupancies were observed for the  $C_{\text{CAAC}}\text{-P}$  bond. Among those, one exhibited polarization towards the  $C_{\text{CAAC}}$  atom, signifying  $\sigma$ -type (62.3%) donation from  $C_{\text{CAAC}}$  to the vacant orbitals of P, while the other indicated  $\pi$ -backdonation (64.9%) from P to  $C_{\text{CAAC}}$ , evident from the HOMO of **2** (Figure 6, top). The higher values of the Wiberg Bond Indices (WBI) [30] ranging from 1.3 to 1.4 for these bonds further corroborate the similar observation as above. The P-P bond exhibited a marginal polarization towards the P atom (55.4%), the one bearing the AuCl group. Notably, the lone pairs were exclusively detected on the P atom without the AuCl group, implying their involvement in bonding with the AuCl group. The HOMO of **2** demonstrated the  $\pi$ -backdonation (64.9%) from P to  $C_{\text{CAAC}}$ , while HOMO-1 indicated the presence of lone pairs on P atoms, and the electron density delocalization between the carbenes. The HOMO-2 showcased the occupied d orbitals of the Au atom (see SI). In contrast, complex **3** exhibited only one bonding occupancy for the  $C_{\text{CAAC}}\text{-P}$  bond, primarily polarized towards the C atoms. This was supported by a slight reduction in the WBI value (1.266) compared to that of **2**, which correlated with a minor elongation of the  $C_{\text{CAAC}}\text{-P}$  bond length in **3**. Moreover, the presence of lone pairs on both P atoms, a feature not seen in **2**, was observed in the case of complex **3**. In complex **5**, the single bond occupancy is observed for both the  $C_{\text{CAAC}}\text{-P}$  bonds, with an absence of lone pairs of electrons on P atoms (Figure 6). Furthermore, the WBI of  $C_{\text{CAAC}}\text{-P}$  bonds (0.971) is found to be reduced compared to that in complexes **2** (1.302/1.441), and **3** (1.266). This strongly suggests the involvement of the lone pairs on P atoms in the bonding with AuCl moiety, resulting in an increased  $C_{\text{CAAC}}\text{-P}$  bond length (1.843(9) to 1.850(10) Å). Additionally, the presence of the aurophilic interactions is visually confirmed in the HOMO-31 of complex **5** (see SI, Figure S11).

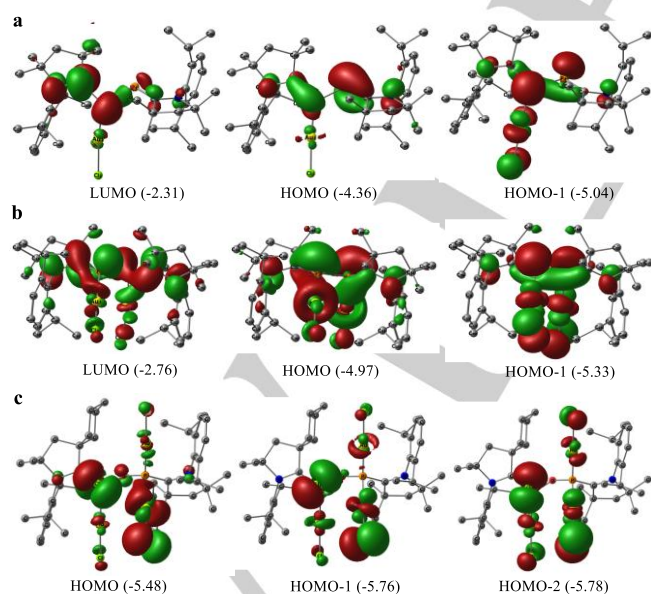


**Figure 6.** The natural bond orbitals (NBOs) of complexes **2** (a), **3** (b) and **5** (c) obtained at BP86-D3(BJ)/def2-TZVPP level of theory (energies given in parentheses are in eV).

The atoms-in-molecules (AIM) analysis<sup>[31]</sup> on complex **5** was performed using the BP86/def2-TZVPP level of theory, which significantly illustrated a bond path and a clear bond critical point (BCP) between the Au1 and Au3 atoms, as indicated by the respective green dot in Figure 7. This observation also proves the presence of the aurophilic interaction between Au1 and Au3 atoms in complex **5**. The second-order perturbation analysis reveals that the interaction between the Au1-Au3-Cl5 bond and the Au1-P7 antibond are the most significant factors contributing to the overall stabilization of the species with an energy value of 104.22 kcal/mol. Additionally, the interaction between the Au1-Au3-Cl5 bond and the Rydberg-type acceptor orbitals on Au1 with a stabilization energy of approximately 65 kcal/mol is also observed.

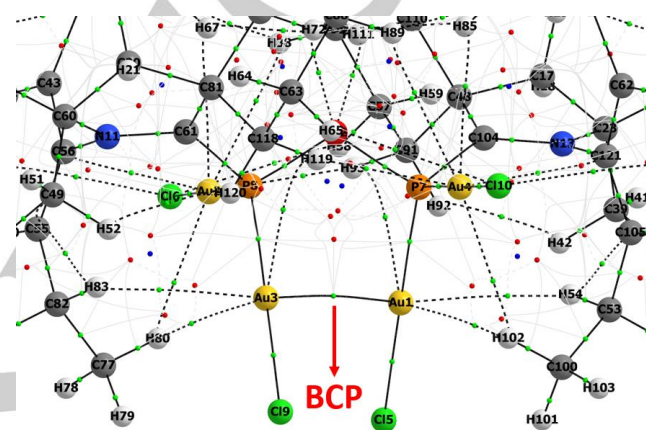
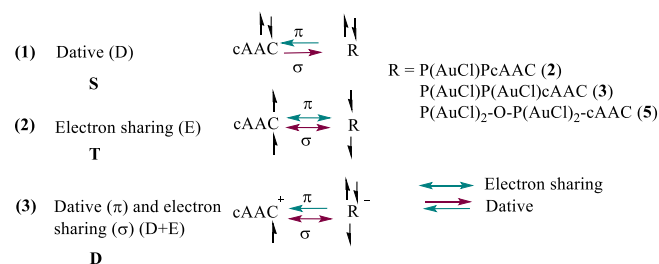


**Figure 7.** Topological map showing bond paths and bond critical points (BCP) of complex **5**.

The energy decomposition analysis coupled with natural orbital for chemical valence (EDA-NOCV) [32] was performed to study the nature of the bond between cAAC and P atoms of bis-(cAAC)-supported di-phosphorus compound **1**, and complexes **2-3, 5** (see SI). Initially, the bond between P and  $C_{\text{CAAC}}$  was broken, giving rise to cAAC and P(AuCl)PcAAC/P(AuCl)P(AuCl)cAAC/P(AuCl)<sub>2</sub>-O-P(AuCl)<sub>2</sub>-cAAC for complexes **2/3/5**, respectively. EDA-NOCV analyses was performed on these fragments to obtain the best bonding description by changing the spin and charge, creating different bonding possibilities (Scheme 2).



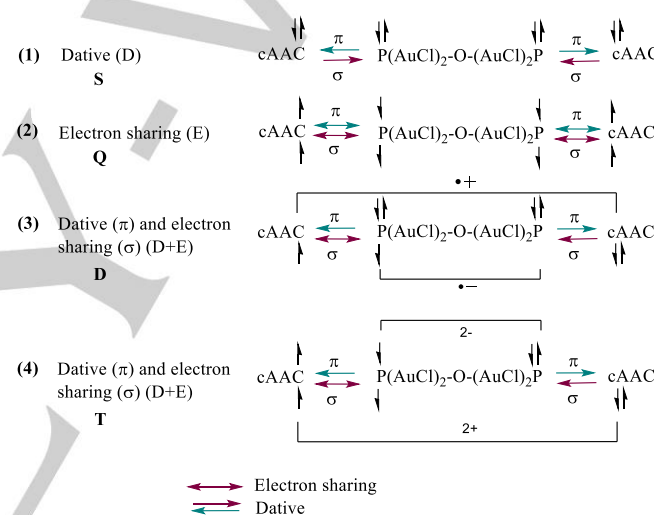
**Scheme 2.** Possible bonding scenarios analyzed for complexes **2-3, 5**.

The first bonding possibility defines a dative bond formed between the neutral and singlet fragments ( $C_{\text{CAAC}}$  and P atoms). The second bonding possibility is the interaction of the neutral and triplet state fragments, forming electron-sharing bonds

between the fragments. The third possibility is considering the interaction of the singly charged doublet fragments creating electron sharing  $\sigma$ -bond and dative  $\pi$ -bonds. However, the best bonding is described by the least  $\Delta E_{\text{orb}}$  (see SI). The bond between cAAC and P(AuCl)PcAAC/ P(AuCl)P(AuCl)cAAC fragments for complexes **2/3**, respectively could be best described when the fragments interact in a neutral triplet state forming the electron sharing bond (see SI, Figures S16-17). The major contribution to the attractive forces is from  $\Delta E_{\text{orb}}$  (~54%).  $\Delta E_{\text{elstat}}$  contributes only 39.7% and 38.4%, respectively for **2** and **3**.  $\Delta E_{\text{orb}}$  further can be divided into pairwise interactions of the fragments. The major contribution to the total  $\Delta E_{\text{orb}}$  is from the electron sharing  $\sigma$ -bond ( $\Delta E_{\text{orb}(1)}$ ) (61.5% (**2**); 58.6% (**3**)).  $\Delta E_{\text{orb}(2)}$  is due to the formation of electron sharing  $\pi$ -bond. The pairwise interaction of fragments reveals that the contribution from  $\sigma$  orbitals is more than  $\pi$  orbitals to the covalent bonding. Overall, EDA-NOCV analysis predicts an electron-sharing bond between  $C_{\text{cAAC}}$  and P in compound **1**, and complexes **2-3**. The  $\sigma$ -electron sharing bond in compound **1** (66.8%) was found to have the largest contribution to the total  $\Delta E_{\text{orb}}$  compared to that in **2** (61.5%), and **3** (58.6%). Conversely, the  $\pi$ -electron sharing contribution in compound **1** (21.2%) was observed to be the smallest compared to that in **2** (24.7%), and **3** (27.0%).

To understand the bonding situation in the bis-cAAC-stabilized di-phosphorus monoxide-Au complex [(Cy-cAAC=P)-O-(P=cAAC-Cy)(AuCl)<sub>4</sub>] (**5**), we first optimized and performed the NBO analyses of the elusive monomeric species POP at the BP86-D3(BJ)/def2-TZVPP level of theory. The electronic structure studied through NBO analysis of the POP moiety in the singlet state reveals the presence of two bonding occupancies between the P atoms, which is of p character, equally polarized towards both the P atoms. This can be clearly visualized in HOMO, and HOMO-1 of POP moiety (see SI). The HOMO of POP represents the  $\pi$  type orbitals, and the LUMO corresponds to the antibonding of the  $\pi_{\text{P-P}}$  bond. The HOMO-1 orbital shows the  $\sigma$ -type interaction between the P atoms, and the HOMO-2 represents the lone pair on P atoms, which is of majorly s character. The calculated bond length of P-P is 2.422 Å is too long to consider a double bond. We assumed that the addition of cAAC ligands on the P atoms would lead to the cleavage of the P-P bonds and the generation of two p-type lone pairs on P atoms. In light of this, we next optimized the geometry of the donor-base-stabilized di-phosphorus monoxide cAAC-POP-cAAC (**5-4AuCl**), and performed the NBO analysis at BP86-D3(BJ)/def2-TZVPP level of theory to study the electronic nature. Two bonding occupancies were observed for the  $C_{\text{cAAC}}\text{-P}$  bond; one exhibited polarization towards the C atom, signifying the  $\sigma$ -type donation from  $C_{\text{cAAC}}$  to the vacant orbitals of P (HOMO-2), while the other indicated  $\pi$ -backdonation from P to  $C_{\text{cAAC}}$ , evident from the HOMO (see SI). The higher values of Wiberg Bond Indices (WBI) of 1.5 for these bonds further corroborate this observation. Notably, lone pairs were detected on P atoms, which are majorly of s-character. The presence of the lone pair on P atoms further led us to study the reactivity of cAAC-POP-cAAC with AuCl in the form of the isolated complex [(Cy-cAAC=P)-O-(P=cAAC-Cy)(AuCl)<sub>4</sub>] (**5**). The EDA-NOCV analysis was performed to investigate the nature of the bond between the  $C_{\text{cAAC}}$  and the P atom in **5**. Compared to compound **1**, and complexes **2-3**; complex **5** has

the best-described bond between the fragments cAAC and P(AuCl)<sub>2</sub>-O-P(AuCl)<sub>2</sub>-cAAC, which is formed by the interaction of singly-charged doublet fragments and involves  $\sigma$ -electron sharing and  $\pi$ -dative bonds. Notably, the  $\sigma$ -electron sharing bond ( $\Delta E_{\text{orb}(1)}$ ) is the most significant contributor to the total  $\Delta E_{\text{orb}}$ , accounting for 72.1% in **5**. Meanwhile,  $\Delta E_{\text{orb}(2)}$  represents the contribution from  $\pi$ -backdonation (10.1%). Upon cleavage of both the bonds between P and  $C_{\text{cAAC}}$  atoms resulted in the formation of [cAAC cAAC] and [P(AuCl)<sub>2</sub>-O-P(AuCl)<sub>2</sub>] fragments (see SI). Among the various bonding possibilities tried, the first one entails a dative bond formation between the neutral and singlet fragments. The second possibility involves the interaction between neutral and quintet state fragments, resulting in an electron-sharing bond between the fragments. The third and fourth possibilities consider the interaction of singly charged doublet fragments and doubly charged triplet fragments, leading to the formation of a combination of both  $\sigma$ -electron sharing and  $\pi$ -dative bonds (Scheme 3).



**Scheme 3.** Possible bonding scenarios of complex **5**.

The determination of the optimal bonding description relies on minimizing  $\Delta E_{\text{orb}}$ . The bond between [cAAC cAAC] and [P(AuCl)<sub>2</sub>-O-P(AuCl)<sub>2</sub>] fragments is best described when the doubly charged triplet fragments interact to form  $\sigma$ -electron sharing and  $\pi$ -dative bonds. The primary contribution to the attractive forces is almost equally attributed to  $\Delta E_{\text{orb}}$  and  $\Delta E_{\text{elstat}}$ , which constitute approximately 92% of the overall energy and the remaining is contributed by  $\Delta E_{\text{dis}}$  (8%). The  $\Delta E_{\text{orb}}$  can be further dissected into pairwise interactions between the fragments. Notably, the  $\sigma$ -electron sharing bond ( $\Delta E_{\text{orb}(1)}$  and  $\Delta E_{\text{orb}(2)}$ ) makes the most significant contribution to the total  $\Delta E_{\text{orb}}$ , accounting for 73.4% in **5**. On the other hand,  $\Delta E_{\text{orb}(3-4)}$  represents the contribution from  $\pi$  backdonation (9.8%) (Table 1).

The best bonding possibility was when the fragments interacted in a doubly charged triplet state (Figure 8). In comparison with **5**, the best bonding of C and P in **2**, and **3** was when the fragments interacted in a triplet neutral state forming an electron-sharing bond.

**Table 1.** The EDA-NOCV results of C<sub>cAAC</sub>-P bonds of **5** [cAAC cAAC]<sup>2+</sup> and [P(AuCl)<sub>2</sub>-O-P(AuCl)<sub>2</sub>]<sup>2-</sup> (**5**) in the electronic triplet (T) states as interacting fragments at the BP86/def2-TZVP level of theory. Energies are in kcal/mol.

Energy	Interaction	[cAAC cAAC] <sup>2+</sup> (T) + [P(AuCl) <sub>2</sub> -O-P(AuCl) <sub>2</sub> ] <sup>2-</sup> (T)
<b>Complex</b>		<b>5</b>
$\Delta E_{\text{int}}$		-460.61
$\Delta E_{\text{Pauli}}$		718.02
$\Delta E_{\text{disp}}^{\text{[a]}}$		-93.05 (7.9%)
$\Delta E_{\text{elstat}}^{\text{[a]}}$		-595.24 (50.5%)
$\Delta E_{\text{orb}}^{\text{[a]}}$		-490.34 (41.6%)
$\Delta E_{\text{orb}(1)}^{\text{[b]}}$	cAAC-P(AuCl) <sub>2</sub> -O-P(AuCl) <sub>2</sub> -cAAC $\sigma$ -electron sharing	-183.3 (38.3%)
$\Delta E_{\text{orb}(2)}^{\text{[b]}}$	cAAC-P(AuCl) <sub>2</sub> -O-P(AuCl) <sub>2</sub> -cAAC $\sigma$ -electron sharing	-172.3 (35.1%)
$\Delta E_{\text{orb}(3)}^{\text{[b]}}$	cAAC←P(AuCl) <sub>2</sub> -O-P(AuCl) <sub>2</sub> →cAAC $\pi$ -backdonation	-28.1 (5.6%)
$\Delta E_{\text{orb}(4)}^{\text{[b]}}$	cAAC←P(AuCl) <sub>2</sub> -O-P(AuCl) <sub>2</sub> →cAAC $\pi$ -backdonation	-21.0 (4.2%)
$\Delta E_{\text{orb}(\text{rest})}$		-82.7 (16.8%)

<sup>a</sup>The values in the parentheses show the contribution to the total attractive interaction  $\Delta E_{\text{disp}} + \Delta E_{\text{elstat}} + \Delta E_{\text{orb}}$ . <sup>b</sup>The values in parentheses show the contribution to the total orbital interaction  $\Delta E_{\text{orb}}$ .

The amount of  $\pi$  backdonation in **2** (24.7%), and **3** (27%) was found to be larger compared to **5** (10.1%). This observation is corroborated by NBO analysis, which indicates the absence of lone pairs on P in complex **5**.

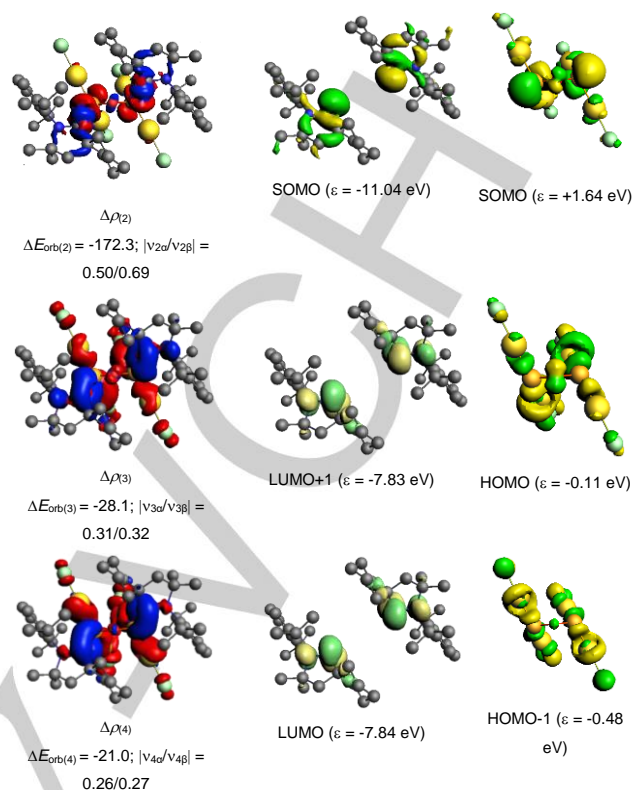
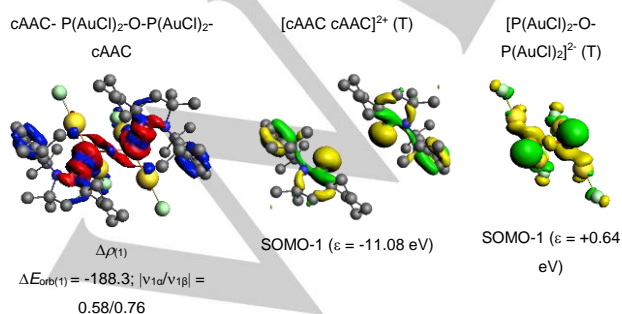
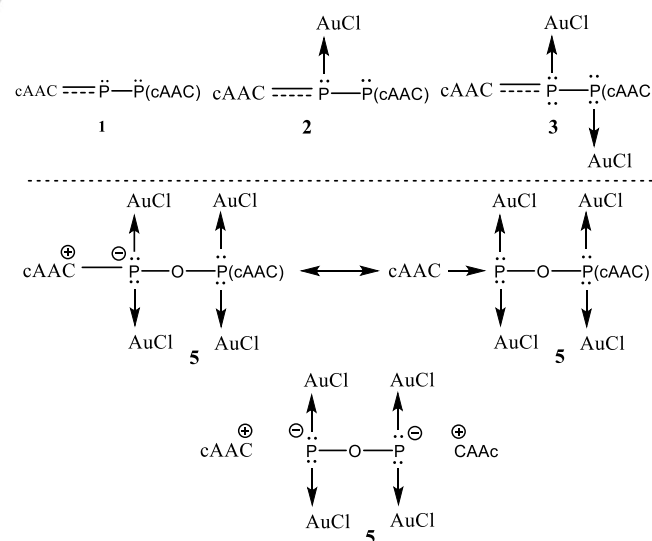


**Figure 8.** The shapes of the deformation densities  $\Delta\rho_{(1)-(4)}$  that correspond to  $\Delta E_{\text{orb}(1)-(2)}$ , and the associated MOs of [(Cy-cAAC=P)-O-(P=cAAC-Cy)(AuCl)<sub>4</sub>] (**5**) and the fragments orbitals [cAAC cAAC]<sup>2+</sup> and [P(AuCl)<sub>2</sub>-O-P(AuCl)<sub>2</sub>]<sup>2-</sup> in the triplet state at the BP86-D3(BJ)/TZ2P level. Isosurface values are 0.001 au for  $\Delta\rho_{(1-2)}$  and isosurface value 0.0003 for  $\Delta\rho_{(3-4)}$ . The eigenvalues  $|v_n|$  give the size of the charge migration in e. The direction of the charge flow of the deformation densities is red→blue.

Compared to **1**, **2**, and **3**, complex **5** has the best-described bond between cAAC and P(AuCl)<sub>2</sub>-O-P(AuCl)<sub>2</sub>-cAAC, which is formed by the interaction of singly charged doublet fragments and involves  $\sigma$ -electron sharing and  $\pi$ -dative bonds (Scheme 4).



**Scheme 4.** The best bonding scenarios of compound **1**, and complexes **2-3**, **5**.

Overall, the EDA-NOCV analysis suggests the presence of an electron-sharing bond between  $C_{cAAC}$  and  $P(AuCl)PcAAC/P(AuCl)P(AuCl)cAAC$ , evidenced by the observed minimal  $\Delta E_{orb}$ . Additionally, from the NBO analysis, a distinctive lone pair is discernible on the phosphorus atom bearing AuCl in **3** with an occupancy of 1.65, whereas, it is absent on the phosphorus atom bearing AuCl in **2**. This disparity accounts for the slight reduction in bond length observed in  $C_{cAAC}$  and P in **2** compared to **3**. In contrast to complexes **2** and **3**, EDA-NOCV predicts a combination of electron sharing and dative bonding between  $C_{cAAC}$  and P in **5**. Notably, it is worth mentioning that **5** may also be characterized in terms of dative bonds, given the marginal  $\Delta E_{orb}$  discrepancy between the two potential bonding scenarios (Scheme 4).

## Conclusion

In conclusion, we have established a new synthetic strategy for synthesizing the bis-cAAC-stabilized di-phosphorus ( $cAAC=P$ )<sub>2</sub> (**1**) in a much-improved yield of 68-75% by the reductive dehalogenation of chloro-phosphinidenes and further studied the coordination chemistry with AuCl for the first time. Reaction of **1** with AuCl in a 1:1 and 1:2 molar ratios afforded the pure crystals of mono- and di-aurated P<sub>2</sub> complexes [(Me<sub>2</sub>-cAAC)-P(AuCl)P-(Me<sub>2</sub>-cAAC)] (**2**), and [(Me<sub>2</sub>-cAAC)-P(AuCl)P(AuCl)-(Me<sub>2</sub>-cAAC)] (**3**) complexes, respectively. The elusive bis-cAAC-supported di-phosphorus monoxide has been stabilized for the first time, and isolated in the solid state in the corresponding tetra-aurated form [(Cy-cAAC=P)-O-(P=cAAC-Cy)(AuCl)<sub>4</sub>] (**5**) in moderate yield. Quantum chemical calculations including DFT and EDA-NOCV analyses revealed the electron sharing  $\sigma$  (61.5% (**2**); 58.6% (**3**)) and  $\pi$  (24.7% (**2**); 27.0% (**3**)) bonds between the  $C_{cAAC}$  and the P atoms in complexes **2**, **3**. Whereas, the results of EDA-NOCV analyses for complex **5** revealed the least  $\Delta E_{orb}$  for the fragments orbitals  $[cAAC\ cAAC]^{2+}$  and  $[P(AuCl)_2-O-P(AuCl)_2]^{2-}$  in the triplet state comprising the most favorable bonding interaction between the donor base ligands, i.e., cAAC and the central (AuCl)<sub>2</sub>POP(AuCl)<sub>2</sub> as the (73.4%) electron-sharing  $\sigma$ -bond ( $\Delta E_{orb(1-2)}$ ) with a smaller contribution (9.8%) of  $\pi$ -backdonation ( $\Delta E_{orb(3-4)}$ ) from the HOMO of  $[P(AuCl)_2-O-P(AuCl)_2]^{2-}$  into the LUMO of the  $[cAAC\ cAAC]^{2+}$ .

## Experimental Section

All manipulations were carried out using either standard Schlenk line techniques under an argon atmosphere or in an argon-filled glove box, where O<sub>2</sub> and H<sub>2</sub>O levels were kept below 0.1 ppm at all times using oven-dried (150 °C) glassware. Solvents obtained from the Solvent Purification System were further dried by refluxing with Na/K alloy for two days, followed by vacuum distillation over 4 Å molecular sieves. Commercially purchased deuterated solvent CD<sub>2</sub>Cl<sub>2</sub> was further purified by stirring over anhydrous CaH<sub>2</sub> for two days, followed by 12 h of reflux, and vacuum distillation.

**Synthesis of complex [(Me<sub>2</sub>-cAAC=P)<sub>2</sub>(AuCl)] (**2**):** In an oven-dried Schlenk flask, [Me<sub>2</sub>-cAAC=P]<sub>2</sub> (140 mg, 0.22 mmol, 1 equiv), and anhydrous (Me<sub>2</sub>S)AuCl (65 mg, 0.22 mmol, 1 equiv) were taken. Added freshly distilled toluene (25 mL) at rt to obtain a clear orange solution, and stirred overnight in the absence of light. Then the reaction mixture was concentrated under reduced pressure to remove the solvent. The orange sticky solid obtained was further dissolved in anhydrous DCM. The resulting orange color clear solution was concentrated up to 1-2 mL, and stored at -32 °C. The block-shaped orange crystals, suitable for X-ray single-crystal diffraction were formed after 4-5 days (90 mg, 47%) from a -32 °C freezer.

**<sup>1</sup>H NMR** (400 MHz, 298 K, DCM-*d*<sub>2</sub>)  $\delta$ : 7.40 (t, *J* = 7.8 Hz, 2H, -ArH), 7.24 (d, *J* = 7.8 Hz, 4H, -ArH), 2.76 (h, *J* = 6.6 Hz, 4H, -CH(CH<sub>3</sub>)<sub>2</sub>), 2.11 (s, 4H, -CH<sub>2</sub>), 1.78 (s, 12H, -CH<sub>3</sub>), 1.42 (d, *J* = 6.8 Hz, 12H, -CH(CH<sub>3</sub>)<sub>2</sub>), 1.27-1.21 (m, 24H, -CH(CH<sub>3</sub>)<sub>2</sub>) ppm; **<sup>31</sup>P NMR** (162 MHz, 253 K, DCM-*d*<sub>2</sub>)  $\delta$ : 36.2 (d, *J* = 294.8 Hz), 12.52, -4.1 (d, *J* = 312.1 Hz) ppm; **<sup>13</sup>C {<sup>1</sup>H} NMR** (101 MHz, 298 K, DCM-*d*<sub>2</sub>)  $\delta$ : 208.4 (d, *J*<sub>C-P</sub> = 22.0 Hz), 147.5, 133.9, 129.7, 125.9, 55.6, 52.1, 29.9 (8.0 Hz), 29.7, 29.1, 27.3, 24.6 ppm; **M.P.** 194-196 °C.

**Synthesis of complex [(Me<sub>2</sub>-cAAC=P)<sub>2</sub>(AuCl)<sub>2</sub>] (**3**):** In an oven-dried Schlenk flask, [Me<sub>2</sub>-cAAC=P]<sub>2</sub> (140 mg, 0.22 mmol, 1 equiv), and anhydrous (Me<sub>2</sub>S)AuCl (130 mg, 0.44 mmol, 2 equiv) were taken. Added freshly distilled toluene (25 mL) at rt to obtain a clear yellowish-orange solution and stirred overnight in the absence of light. The orange color precipitate was formed after overnight stirring. Then the reaction mixture was filtered through a frit to obtain the orange color residue and the filtrate. The residue (110 mg, 45%) was further washed with *n*-hexane, and dissolved in anhydrous DCM. The orange-yellow solution was concentrated up to 1-2 mL, and stored at -32 °C. The block-shaped golden yellow crystals, suitable for X-ray single-crystal diffraction were formed in 4-5 days.

**<sup>1</sup>H NMR** (400 MHz, 298 K, DCM-*d*<sub>2</sub>)  $\delta$ : 7.50 (t, *J* = 7.8 Hz, 2H, -ArH), 7.29 (d, *J* = 7.8 Hz, 4H, -ArH), 2.63 (s, 4H, -CH(CH<sub>3</sub>)<sub>2</sub>), 2.21 (s, 4H, -CH<sub>2</sub>), 1.89 (s, 12H, -CH<sub>3</sub>), 1.58 (d, *J* = 6.6 Hz, 12H, -CH(CH<sub>3</sub>)<sub>2</sub>), 1.33 (s, 12H, -CH<sub>3</sub>), 1.24 (d, *J* = 6.6 Hz, 12H, -CH(CH<sub>3</sub>)<sub>2</sub>) ppm; **<sup>31</sup>P NMR** (162 MHz, 298 K, DCM-*d*<sub>2</sub>)  $\delta$ : 14.8 ppm; **<sup>13</sup>C {<sup>1</sup>H} NMR** (101 MHz, 298 K, DCM-*d*<sub>2</sub>)  $\delta$ : 209.3 (d, *J*<sub>C-P</sub> = 11.0 Hz), 147.8, 133.5, 130.8, 129.3, 128.5, 125.6, 75.4, 30.1, 29.4, 25.0 ppm; **M.P.** 170-172 °C.

**Synthesis of complex [(Cy-cAAC=P)-O-(P=cAAC-Cy)(AuCl)<sub>4</sub>] (**5**):** In an oven-dried Schlenk flask, [Cy-cAAC=P-B(N-(*i*-Pr)<sub>2</sub>)<sub>2</sub>] (**4**, 250 mg, 0.43 mmol, 1 equiv), and (Me<sub>2</sub>S)AuCl (294.5 mg, 0.86 mmol, 2 equiv) were taken. Added freshly distilled toluene (25 mL) at rt to obtain a clear yellowish-orange solution, and stirred overnight in the absence of light. The brownish-orange color precipitate was formed after overnight stirring. Then the reaction mixture was filtered through a frit to obtain a brownish-orange color residue. The residue of complex **5** (50 mg, 15%) was further washed with *n*-hexane, and dissolved in anhydrous THF. The golden yellow reaction mixture

was concentrated up to 1-2 mL, opened in the air for a few seconds and then stored at a -32 °C freezer. The golden yellow blocks of **5**, suitable for X-ray single-crystal diffraction were formed in 1-2 days along with deposition of the brown precipitate.

<sup>1</sup>H NMR (400 MHz, 298 K, DMSO-*d*<sub>6</sub>) δ: 7.49-7.44 (m, 2H, -ArH), 7.27-7.22 (m, 2H, -ArH), 7.19-7.14 (m, 2H, -ArH), 3.32 (br, 4H, -CH(CH<sub>3</sub>)<sub>2</sub>), 2.71 (s, 2H, -cyclohexyl), 2.68-2.61 (m, 4H, -cyclohexyl), 2.40-2.36 (m, 4H, -CH<sub>2</sub>), 2.01 (d, *J* = 12.4 Hz, 2H, -cyclohexyl), 1.57 (d, *J* = 6.5 Hz, 4H, -cyclohexyl), 1.49 (d, *J* = 12.8 Hz, 6H, -cyclohexyl), 1.40-1.36 (m, 12H, -CH(CH<sub>3</sub>)<sub>2</sub>), 1.32 (s, 2H, -cyclohexyl), 1.29-1.23 (m, 18H, -CH(CH<sub>3</sub>)<sub>2</sub>), 1.22 (s, 3H, -CH<sub>3</sub>), 1.20 (s, 3H, -CH<sub>3</sub>) ppm; <sup>31</sup>P NMR (162 MHz, 298 K, DMSO-*d*<sub>6</sub>) δ: -80.9 ppm; <sup>13</sup>C {<sup>1</sup>H} NMR (101 MHz, 298 K, DMSO-*d*<sub>6</sub>) δ: 138.2, 129.2, 128.6, 128.4, 125.5, 60.0, 31.9, 30.0, 29.6, 25.9, 22.9, 19.9, 14.2 ppm. M.P. 215-217 °C.

**Crystallographic details:** The single-crystal X-ray data for complexes **2-3**, **5** were collected on a Bruker D8 VENTURE diffractometer equipped with PHOTON III C28 detector using  $\lambda$   $\mu$ S 3.0 microfocus sealed X-ray source with Molybdenum K $\alpha$  ( $\lambda$  = 0.71073 Å) radiation. Complete data set was collected following the strategies generated using the APEX4<sup>[33]</sup> module of the Bruker software suite. The data reduction was carried out using SAINTPLUS,<sup>[33]</sup> and multi-scan absorption correction was performed using the program SADABS.<sup>[33]</sup> The crystal structures were solved by the intrinsic phasing method (SHELXT),<sup>[34]</sup> and were refined with full-matrix least squares on F<sup>2</sup> using ShelXle<sup>[35]</sup> plug-in included in APEX4. All non-hydrogen atoms were refined anisotropically. OLEX2 Version 1.3.0 was used for structure solution and refinement.<sup>[36]</sup> Ortep-3 was used to produce the thermal ellipsoid plots of all the structures.<sup>[37]</sup>

## Supporting Information

Deposition Numbers 2278346 (for **2**), 2278347 (for **3**), and 2278348 (for **5**) contain the supplementary crystallographic data for this paper. The Crystallographic Information Files for **2-3**, **5** can be obtained from the joint Cambridge Crystallographic Data Centre and Fachinformationszentrum Karlsruhe Access Structures service via [www.ccdc.cam.ac.uk/structures/](http://www.ccdc.cam.ac.uk/structures/).

## Acknowledgments

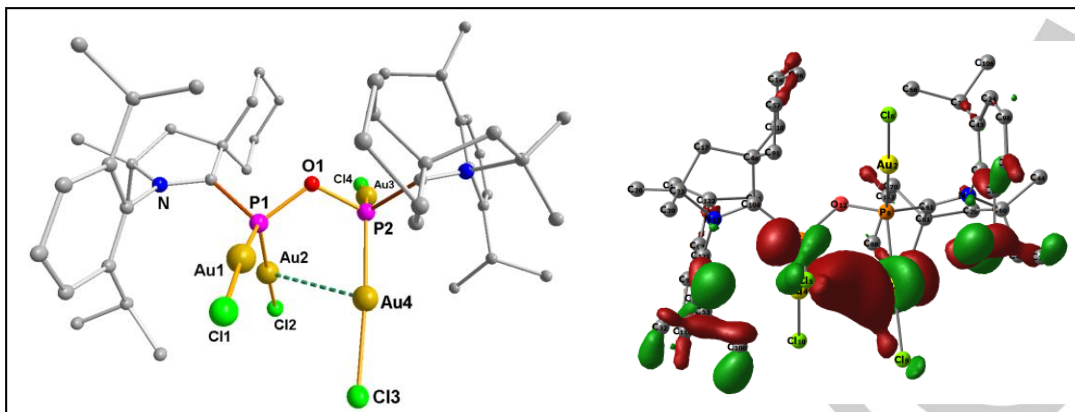
SR gratefully acknowledges SERB, New Delhi for the POWER grant (SPG/2021/003237); STARS, MoE, Govt. of India (MoE-STARS/STARS-2/2023-0666); and IISER Tirupati. MF and EN thank CSIR and IISER Tirupati for their respective SRF. We thank Dr. P. K. Sudhadevi Antharjanam (SAIF-IITM) for her valuable suggestions during the structure refinement of complex **5**.

**Keywords:** Au(I)-complexes • Auophilic interaction • Diphosphorus monoxide • Cyclic alkyl(amino) carbene • Structure and bonding

- (a) Jr. M. W. Chase, **1998**. NIST-JANAF Thermochemical Tables (Fourth Edition). (b) H. Bock, H. Mueller, *Inorg. Chem.*, **1984**, *23*, 4365-4368. (c) D. Tofan, C. C. Cummins, *Angew. Chem. Int. Ed.*, **2010**, *49*, 7516-7518.
- (a) Y. Wang, Y. Xie, P. Wei, K. R. Bruce, H. F. Schaefer, III, P. v. R. Schleyer, G. H. Robinson, *J. Am. Chem. Soc.*, **2008**, *130*, 14970-14971. (b) O. Back, G. Kuchenbeiser, B. Donnadieu, G. Bertrand, *Angew. Chem. Int. Ed.*, **2009**, *48*, 5530-5533. (c) T. J. Hadlington, A. Kostenko, M. Driess, *Chem. Eur. J.*, **2021**, *27*, 2476-2482. (d) Y. Wang, T. Szilvási, S. Yao, M. Driess, *Nature Chemistry*, **2020**, *12*, 801-807. (e) J. Sun, H. Verplancke, J. I. Schweizer, M. Diefenbach, C. Würtele, M. Otte, I. Tkach, C. Herwig, C. Limberg, S. Demeshko, M. C. Holthausen, S. Schneider, *Chem*, **2021**, *7*, 1952-1962. (f) S. Asami, M. Okamoto, K. Suzuki, M. Yamashita, *Angew. Chem. Int. Ed.*, **2016**, *55*, 12827-12831. (g) L. L. Liu, L. L. Cao, J. Zhou, D. W. Stephan, *Angew. Chem. Int. Ed.*, **2019**, *58*, 273-277. (h) S. Lauk, M. Zimmer, B. Morgenstern, V. Huch, C. Müller, H. Sitzmann, A. Schäfer, *Organometallics*, **2021**, *40*, 618-626. (i) D. Rottschäfer, M. K. Sharma, B. Neumann, H. Stammler, D. M. Andrada, Ghadwal, Rajendra S, *Chem. Eur. J.*, **2019**, *25*, 8127-8134. (j) Y. Xiong, S. Yao, T. Szilvási, E. Ballester-Martinez, H. Grützmacher, M. Driess, *Angew. Chem. Int. Ed.*, **2017**, *56*, 4333-4336. (k) N. Holzmann, D. Dange, C. Jones, G. Frenking, *Angew. Chem. Int. Ed.*, **2013**, *52*, 3004-3008. (l) N. Holzmann, D. Dange, C. Jones, G. Frenking, *Angew. Chem. Int. Ed.*, **2013**, *52*, 3004-3008.
- (a) B. M. Cossairt, N. A. Piro, C. C. Cummins, *Chem. Rev.*, **2010**, *110*, 4164-4177. (b) M. Caporali, L. Gonsalvi, A. Rossin, M. Peruzzini, *Chem. Rev.*, **2010**, *110*, 4178-4235. (c) F. Dielmann, M. Sierka, A. Virovets, M. Scheer, *Angew. Chem. Int. Ed.*, **2010**, *49*, 6860-6864. (d) B. Zarzycki, T. Zell, D. Schmidt, U. Radius, *Eur. J. Inorg. Chem.*, **2013**, *2013*, 2051-2058. (e) S. Yao, T. Szilvási, N. Lindenmaier, Y. Xiong, S. Inoue, M. Adelhardt, J. Sutter, K. Meyer, M. Driess, *Chem. Commun.*, **2015**, *51*, 6153-6156.
- L. Weber, U. Lassahn, H. Stammler, B. Neumann, *Eur. J. Inorg. Chem.*, **2005**, *2005*, 4590-4597.
- (a) F. A. Cotton, G. Wilkinson, C. Murillo, M. Bochmann, *Advanced Inorganic Chemistry*, 6th ed.; Wiley: New York, **1999**. (b) F. G. A. Stone, R. West, Eds. *Advances in Organometallic Chemistry*, Volume 42; Academic Press: San Diego, **1998**.
- N. A. Piro, J. S. Figueroa, J. T. McKellar, C. C. Cummins, *Science*, **2006**, *313*, 1276-1279.
- N. A. Piro, C. C. Cummins, *Inorg. Chem.*, **2007**, *46*, 7387-7393.
- (a) Y. Wang, Y. Xie, M. Y. Abraham, P. Wei, H. F. Schaefer III, P. v. R. Schleyer, G. H. Robinson, *Chem. Commun.*, **2011**, *47*, 9224-9226. (b) Y. Wang, H. P. Hickox, Y. Xie, P. Wei, D. Cui, M. R. Walter, H. F. Schaefer III, G. H. Robinson, *Chem. Commun.*, **2016**, *52*, 5746-5748.
- Y. Wang, Y. Xie, M. Y. Abraham, R. J. Jr, P. Wei, H. F. Schaefer III, P. v. R. Schleyer, G. H. Robinson, *Organometallics*, **2010**, *29*, 4778-4780.
- Y. Wang, Y. Xie, P. Wei, H. F. Schaefer III, P. v. R. Schleyer, G. H. Robinson, *J. Am. Chem. Soc.*, **2013**, *135*, 19139-19142.
- R. B. Schlesinger, In *Environmental Toxicants: Human Exposures and Their Health Effects*; 3rd ed.; Lippmann, M., Ed.; John Wiley & Sons, Inc.: Hoboken, NJ, **2008**.
- Z. Mielke, M. McCluskey, L. Andrews, *Chem. Phys. Lett.*, **1990**, *165*, 146.
- O. J. Scherer, J. Braun, P. Walther, G. Heckmann, G. Wolmershaeuser, *Angew. Chem., Int. Ed. Engl.*, **1991**, *30*, 852.
- O. J. Scherer, S. Weigel, G. Wolmershauser, *Angew. Chem., Int. Ed.*, **1999**, *38*, 3688.
- S. Roy, K. C. Mondal, S. Kundu, B. Li, C. J. Schürmann, S. Dutta, D. Koley, R. Herbstlirmer, D. Stalke, H. W. Roesky, *Chem. Eur. J.*, **2017**, *23*, 12153-12157.
- A. Kulkarni, S. Arumugam, M. Francis, P. G. Reddy, E. Nag, S. M. N. V. T. Gorantla, K. C. Mondal, S. Roy, *Chem. Eur. J.* **2021**, *27*, 200-206.
- E. Nag, S. Battuluri, B. B. Sinu, S. Roy, *Inorg. Chem.* **2022**, *61*, 13007-13014.
- E. Nag, S. Battuluri, K. C. Mondal, S. Roy, *Chem. Eur. J.* **2022**, *28*, e202202324.
- E. Nag, M. Francis, S. Roy, *Eur. J. Inorg. Chem.*, **2023**, e202300485.
- D. V. Partyka, M. P. Washington, T. G. Gray, James, J. F. II, J. D. Protasiewicz, *J. Am. Chem. Soc.*, **2009**, *131*, 10041-10048.

- [21] M. Casciotti, G. Romolskas, M. Álvarez, F. Molina, MuñozMolina, José María, Belderrain, Tomás R, L. Rodríguez, *Dalton Trans.*, **2022**, *51*, 17162-17169.
- [22] T. P. Seifert, S. Bestgen, T. J. Feuerstein, S. Lebedkin, F. Krämer, C. Fegler, M. T. Gamer, M. M. Kappes, P. W. Roesky, *Dalton Trans.*, **2019**, *48*, 15427-15434.
- [23] P. Kumar, Kashid, Vitthalrao S, Y. Reddi, J. T. Mague, Sunoj, Raghavan B, Balakrishna, Maravanji S, *Dalton Trans.*, **2015**, *44*, 4167-4179.
- [24] S. Bestgen, M. T. Gamer, S. Lebedkin, M. M. Kappes, P. W. Roesky, *Chem. Eur. J.* **2015**, *21*, 601-614.
- [25] H. Schmidbaur, A. Schier, *Chem. Soc. Rev.*, **2012**, *41*, 370-412.
- [26] F. Flecken, T. Grell, S. Hanf, *Dalton Trans.*, **2022**, *51*, 8975-8985.
- [27] Y. Wang, Y. Xie, P. Wei, H. F. III, Paul, G. H. Robinson, *J. Am. Chem. Soc.* **2013**, *135*, 19139-19142.
- [28] (a) A. D. Becke, *Phys. Rev. A: At., Mol., Opt. Phys.*, **1988**, *38*, 3098-3100; (b) J. P. Perdew, *Phys. Rev. B: Condense. Matter Mater. Phys.*, **1986**, *33*, 8822-8824.
- [29] (a) F. Weinhold and C. Landis, *Valency and Bonding, A Natural Bond Orbital Donor-Acceptor Perspective*, Cambridge University Press, Cambridge, **2005**. (b) C. R. Landis and F. Weinhold, *The NBO View of Chemical Bonding, The Chemical Bond: Fundamental Aspects of Chemical Bonding*, G. Frenking and S. Shaik, Wiley, **2014**, pp. 91-120; (c) A. E. Reed, L. A. Curtiss and F. Weinhold, *Chem. Rev.*, **1988**, *88*, 899-926.
- [30] K. B. Wiberg, *Tetrahedron*, **1968**, *24*, 1083-1096.
- [31] (a) K. Morokuma, *J. Chem. Phys.*, **1971**, *55*, 1236-1244. (b) T. Ziegler and A. Rauk, *Theor. Chim. Acta*, **1977**, *46*, 1-10. (c) M. Mitoraj and A. Michalak, *Organometallics*, **2007**, *26*, 6576-6580. (d) M. Mitoraj and A. Michalak, *J. Mol. Model.*, **2008**, *14*, 681-687. (e) G. te Velde, F. M. Bickelhaupt, E. J. Baerends, C. Fonseca Guerra, S. J. A. van Gisbergen, J. G. Snijders and T. Ziegler, *J. Comput. Chem.*, **2001**, *22*, 931-967
- [32] (a) R. F. Bader, *Atoms in Molecules: A Quantum Theory*, Clarendon Pr, Oxford, **1990**. (b) R. F. W. Bader, *Chem. Rev.*, **1991**, *91*, 893-928. (c) R. F. W. Bader, *Acc. Chem. Res.*, **1985**, *18*, 9-5. (d) C. F. Matta, R. J. Boyd, *The Quantum Theory of Atoms in Molecules: From Solid State to DNA and Drug Design*, Wiley-Vch, Weinheim, **2007**.
- [33] Bruker (**2021**). APEX4. Bruker Nano, Inc., Madison, WI, USA.
- [34] 'SAINT V8.40B (Bruker AXS LLC, **2019**).
- [35] L. Krause, R. Herbst-Irmer, G. M. Sheldrick, D. Stalke, *J. Appl. Cryst.*, **2015**, *48*, 3-10.
- [36] G. M. Sheldrick, *Acta Cryst. Section A: Foundations and Advances*, **2015**, *71*, 3-8.
- [37] C. B. Hübschle, G. M. Sheldrick, B. Dittrich, *J. Appl. Cryst.*, **2011**, *44*, 1281-1284.

## Entry for the Table of Contents



The coordination behavior of the bis-cAAC-stabilized di-phosphorus ( $P_2$ ) has been studied with AuCl. The mono- and di-aurated  $P_2$  complexes have been isolated in the solid state in good yields. The elusive donor-base-stabilized di-phosphorus monoxide has been successfully stabilized, and isolated for the first time in its tetra-aurated form with significant aurophilic interaction. All the Au complexes have been structurally characterized by single-crystal X-ray diffraction and studied further by NMR spectroscopy.

Institute and/or researcher Twitter usernames: @liserTirupati